Investigation on Advanced Receiver Employing Interference Rejection Combining in Asynchronous Network for LTE-Advanced Downlink

Yusuke Ohwatari†, Nobuhiko Miki†, Tetsushi Abe†, and Hidekazu Taoka‡

†NTT DOCOMO, INC.
3-6 Hikari-no-oka, Yokosuka-shi, Kanagawa-ken
239-8536 Japan

‡DOCOMO Communications Laboratories Europe GmbH
Landsberger Strasse 312, 80687, Munich, Germany

***Abstract*- The interference rejection combining (IRC) receiver, which can suppress inter-cell interference, is effective in improving the cell-edge user throughput. The IRC receiver is typically based on the minimum mean square error (MMSE) criteria, which requires highly accurate channel estimation and covariance matrix estimation that includes the inter-cell interference. To do this, the channel estimation and covariance matrix must be averaged within a subframe, i.e., 1 msec. However, the source of the inter-cell interference is changed within one subframe of the covariance matrix estimation due to the change in the user allocation at the interfering cells if asynchronous networks are employed. This affects the performance gain of the IRC receiver. This paper investigates the impact on asynchronous networks and the gain from the IRC receiver in terms of the downlink user throughput performance. Simulation results based on a 57-cell model environment, i.e., a cellular environment in the LTE-Advanced downlink, show that an IRC receiver that has two receiver antenna branches effectively suppresses the inter-cell interference even when asynchronous networks are employed.**

I. INTRODUCTION

The Long-Term Evolution (LTE) was finalized as Release 8 (simply LTE hereafter) by the 3rd Generation Partnership Project (3GPP) [1]. In Japan, NTT DOCOMO launched a commercial LTE service in December 2010 under the new service brand of "Xi" (crossy) [2]. Following the requirements for LTE-Advanced [3], the specifications on LTE-Advanced were initiated as Release 10 and beyond. In LTE-Advanced, to satisfy high-level requirements for the peak and average spectrum efficiency and cell-edge user throughput, advanced multi-antenna transmission techniques such as higher-order single-user (SU)-MIMO, multi-user (MU)-MIMO, and coordinated multi-point (CoMP) transmission/reception were investigated [4]. The interference rejection combining (IRC) receiver [5] was also evaluated [4]. Regarding the IRC receiver, the study item (SI) phase in which fundamental studies are conducted on elemental technologies for LTE-Advanced (Release 11) was initiated [6].

Among these techniques, the advanced receiver employing IRC is effective in improving the cell-edge user throughput. As shown in Fig. 1, the IRC receiver utilizes the correlation of the interference of multiple receiver branches, and combines the received signals for multiple receiver branches so that the mean square error (MSE) between the combined signal and the desired signal is minimized instead of employing maximal ratio combining (MRC) in the case of one stream transmission [7]-[10].

The IRC receiver however, requires knowledge of the interference signals, i.e., the covariance matrix including the interference signals, in addition to the desired signal, i.e., the channel matrix of the serving cell. In a practical application, these matrices should be estimated accurately using the received signals, e.g., the downlink reference signals (RSs) or the data signals, at the IRC receiver. In order to improve the accuracy of these matrices, the averaging operation for these matrices is effective, if the interference statistics are constant. If all the cells are synchronized, i.e., all the cells have the same transmission timing, the interference statistics within the minimum assignment unit, i.e., resource block (RB), are assumed to be the same. This is because the user assignment and precoding matrix from all the surrounding cells are constant within the RB. To clarify the potential gain from the IRC receiver, we compared covariance generation methods and evaluated the user throughput performance in the LTE-Advanced downlink assuming a synchronous network, i.e., best condition for IRC receiver [8]. In this evaluation, the inter-cell interference from the surrounding 56 cells were actually generated in the same way as the desired signals in a link-level simulation so that actual estimation errors could be taken into account. The evaluation results showed that the IRC receiver using the covariance matrix estimation scheme described in [10] improved the cell-edge user throughput compared to the simplified MMSE receiver which approximates the inter-cell interference as additive white Gaussian noise (AWGN).

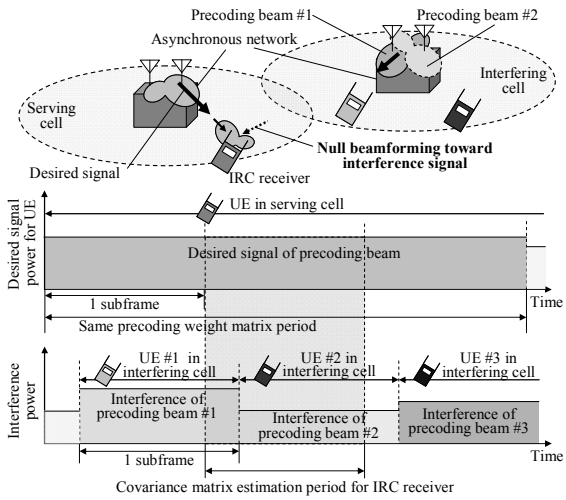

Figure 1. IRC receiver and impact on interference signals in asynchronous network.

The LTE system however, generally assumes an asynchronous network that does not use any inter-site time synchronization, although optimization for synchronous networks is also considered [11]. Therefore, the performance of the IRC receiver should be assessed in an asynchronous network. When asynchronous networks are employed, the source of the inter-cell interference is changed for the averaging period of the covariance matrix estimation due to the change in the user allocation at the interfering cells. Therefore, the estimated covariance matrix becomes inaccurate compared to that in the synchronous network. It is this inaccurate covariance matrix estimation that is expected to cause the

978-1-4673-0990-5/12/$31.00 ©2012 IEEE

performance degradation for the IRC receiver. This paper investigates the impact on asynchronous networks and evaluates the user throughput performance for the IRC receiver employing a multi-cell link simulation as described in [8]. In the investigation, we assume two asynchronous network cases, i.e., only the cells within the same cell site (eNodeB) are synchronized and the cells within a cluster that consists of multiple cells are synchronized. Furthermore, we clarify the performance of the IRC receiver in asynchronous networks assuming the case where the number of interfering cells is limited, i.e., two, three, or four-cell model environment.

In the rest of the paper, Section II describes the detailed structure of the advanced receiver employing the IRC in LTE-Advanced and discusses the impact on asynchronous networks for the receiver. Then, the simulation configuration is given in Section III. Finally, we present the simulation results in Section IV, and our concluding statements in Section V.

II. Interference Rejection Combining Receiver to Suppress Inter-cell Interference

A. Signal Model

The N_{Rx}-dimensional received signal vector of the k-th subcarrier and the l-th OFDM symbol, $\boldsymbol{y}(k,l)$, is expressed as follows.

$$\begin{aligned}\boldsymbol{y}(k,l) &= \sum_{i=0}^{N_{\mathrm{Cell}}-1} \boldsymbol{H}_i(k,l)\boldsymbol{W}_{\mathrm{Tx},i}(k,l)\boldsymbol{s}_i(k,l) + \boldsymbol{n}(k,l) \\ &= \sum_{i=0}^{N_{\mathrm{Cell}}-1} \boldsymbol{G}_i(k,l)\boldsymbol{s}_i(k,l) + \boldsymbol{n}(k,l)\end{aligned}, \quad (1)$$

where $\boldsymbol{H}_i(k,l)$ represents the ($N_{\mathrm{Rx}} \times N_{\mathrm{Tx}}$) channel matrix between the i-th cell and the set of user equipment (UE), $\boldsymbol{W}_{\mathrm{Tx},i}(k,l)$ represents the ($N_{\mathrm{Tx}} \times N_{\mathrm{Stream}}$) precoding weight matrix of the i-th cell, $\boldsymbol{s}_i(k,l)$ represents the N_{Stream}-dimensional information signal vector of the i-th cell, $\boldsymbol{G}_i(k,l)$ is the composite channel defined as $\boldsymbol{H}_i(k,l)\boldsymbol{W}_{\mathrm{Tx},i}(k,l)$, and $\boldsymbol{n}(k,l)$ is the N_{Rx}-dimensional noise vector. Here, N_{Tx}, N_{Stream}, and N_{Cell} are the numbers of transmitter antenna branches at each cell, transmission streams for the UE, i.e., transmission ranks, and the total number of cells, respectively. The 0-th cell ($i = 0$) is defined as the serving cell for the UE. The recovered signal vector at the UE, $\hat{\boldsymbol{s}}_0(k,l)$, is detected by using the ($N_{\mathrm{Stream}} \times N_{\mathrm{Rx}}$) receiver weight matrix $\boldsymbol{W}_{\mathrm{Rx},0}(k,l)$ as follows.

$$\hat{\boldsymbol{s}}_0(k,l) = \boldsymbol{W}_{\mathrm{Rx},0}(k,l)\boldsymbol{y}(k,l). \quad (2)$$

B. IRC Receiver Weight Generation

To obtain the IRC receiver weight matrix, the demodulation RS (DM-RS) based covariance matrix estimation scheme [8][10] is employed. Note that the DM-RS estimates the composite channel matrix of the serving cell, $\boldsymbol{G}_0(k,l)$, to demodulate the data signals without the precoding matrix information. In this scheme, using the DM-RS sequence of the serving cell, which is known at the receiver, the covariance matrix including only the interference and noise component, $\boldsymbol{R}_{I+N}$, is estimated as follows.

$$\boldsymbol{R}_{I+N} = \frac{1}{N_{\mathrm{sp}}} \sum_{l,k \in \boldsymbol{M}_{\mathrm{DMRS}}} \tilde{\boldsymbol{y}}(k,l)\tilde{\boldsymbol{y}}^H(k,l), \quad (3)$$

$$\tilde{\boldsymbol{y}}(k,l) = \boldsymbol{y}(k,l) - \hat{\boldsymbol{G}}_0(k,l)\boldsymbol{p}_0(k,l) \quad (k,l \in \boldsymbol{M}_{\mathrm{DMRS}}), \quad (4)$$

where $\hat{\boldsymbol{G}}_0(k,l)$ is the estimated composite channel based on the DM-RS, $\boldsymbol{p}_0(k,l)$ is the DM-RS sequence of the serving cell, N_{sp} is the number of averaged samples, and $\boldsymbol{M}_{\mathrm{DMRS}}$ is the DM-RS resource element (RE) group. Superscript ^{H} denotes the Hermitian conjugate. Using the estimated $\boldsymbol{R}_{I+N}$ and $\hat{\boldsymbol{G}}_0(k,l)$, the covariance matrix, $\boldsymbol{R}_{yy}(k,l)$, is estimated using the following equation.

$$\boldsymbol{R}_{yy}(k,l) = P_0\hat{\boldsymbol{G}}_0(k,l)\hat{\boldsymbol{G}}_0^H(k,l) + \boldsymbol{R}_{I+N}, \quad (5)$$

where P_0 is the transmit signal power of the serving cell. The IRC receiver weight matrix is calculated using $\boldsymbol{R}_{yy}(k,l)$ as follows.

$$\boldsymbol{W}_{\mathrm{IRC}}(k,l) = P_0\hat{\boldsymbol{G}}_0^H(k,l)\boldsymbol{R}_{yy}^{-1}(k,l). \quad (6)$$

C. Impact on Asynchronous Network for IRC Receiver

Figs. 2(a) and 2(b) show the transmit frame structure of the serving cell and the interfering cell in a synchronous network and asynchronous network when a 2-cell model environment is employed. One RB is shown in the figure, which is the minimum assignment unit defined as 12 subcarriers × 14 OFDM symbols (one subframe). The first two OFDM symbols are assumed to be used for control signaling and the cell specific RS (CRS). The channel state information RS (CSI-RS) is assumed to be multiplexed in the 10th and 11th OFDM symbols. Note that the control signals are transmitted using the space-frequency block code (SFBC) scheme and the CRS is transmitted at each transmit antenna branch. The CSI-RS is transmitted using code division multiplexing (CDM) every two transmit antenna branches. Here, the CRS is the reference signal used to demodulate the control signaling and perform mobility measurement. The CSI-RS is a reference signal used to obtain accurate CSI associated with each transmitter antenna branch. The DM-RS is assumed to be multiplexed with the insertion density of 12 RE/RB. In this section, we assume that the propagation delay is negligible.

Under these assumptions, when assuming a synchronous network as shown in Fig. 2(a), the DM-RSs transmitted with the same precoding weight matrix of the data signals from the interfering cell interfere with all of the DM-RSs transmitted from the serving cell. Therefore, the covariance matrix can be estimated accurately using the DM-RS as mentioned in Section II-B.

On the other hand, in the asynchronous network as shown in Fig. 2(b), different sources of interference may interfere with the DM-RSs transmitted from the serving cell. As shown in Fig. 1, the inter-cell interference is not synchronized with the desired signal. Therefore, two different sources of precoded interference arrive within the covariance matrix estimation period. Since these sources of interference are regarded as interference from two different channels, the number of sources of interference is equivalently increased to generate the IRC receiver weight matrix. Therefore, in the asynchronous network, those sources of interference might impact the throughput performance for the IRC receiver.

Using an example in the asynchronous network as shown in Fig. 2(b), we discuss how the covariance matrix is represented. Note that, in the following investigations, we assume that the transmission timing of the OFDM symbols between the serving cell and the interfering cell is synchronized for simplicity

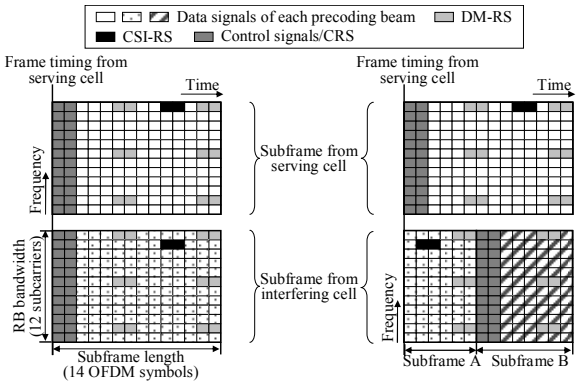

(a) Synchronous network (b) Asynchronous network

Figure 2. Frame structure.

(however, we assume that the transmission timing of the OFDM symbols is not synchronized for the performance evaluation in Section IV). Regarding the example illustrated in Fig. 2(b), the subframes are transmitted from the serving cell and the interfering cell with the delay times of 6 OFDM symbols. In this case, the DM-RSs in the former subframe (Subframe A in the figure) transmitted from the interfering cell interfere with the DM-RSs in the 6th OFDM symbol transmitted from the serving cell. Furthermore, the control signals and CRSs, which are transmitted with non-precoding, in the latter subframe (Subframe B in the figure) from the interfering cell interfere with the DM-RSs in the 7th OFDM symbol from the serving cell. The DM-RSs and precoded data signals in Subframe B interfere with the DM-RSs in the 13th and 14th OFDM symbols from the serving cell. Therefore, the covariance matrix is estimated including three different sources of interference. In principle, if the composite channel matrix of the serving cell, $\boldsymbol{G}_0(k,l)$, can be estimated ideally and the fading fluctuations in the time and frequency domains are negligible, the covariance matrix including only the interference and noise, $\boldsymbol{R}_{I+N}$, is represented as follows.

$$\boldsymbol{R}_{I+N} \cong \frac{1}{4} P_1 \boldsymbol{G}_{1A} \boldsymbol{G}_{1A}^H + \frac{1}{4} P_1 \boldsymbol{H}_1 \boldsymbol{H}_1^H + \frac{1}{2} P_1 \boldsymbol{G}_{1B} \boldsymbol{G}_{1B}^H + \sigma^2 \boldsymbol{I} , \qquad (7)$$

where P_1, σ^2, and $\boldsymbol{I}$ are the transmit signal power of the interfering cell, the noise power, and the ($N_{\mathrm{Rx}} \times N_{\mathrm{Rx}}$) identity matrix, respectively. Terms $\boldsymbol{G}_{1A}$ and $\boldsymbol{G}_{1B}$ represent the composite channels of each subframe from the interfering cell illustrated in Fig. 2(b). The IRC receiver using (7) suppresses the three sources of interference if the degrees of freedom at the receiver are higher than these three sources of interference; otherwise, the performance of the IRC receiver is degraded.

III. Simulation Conditions

To investigate the performance obtained using the IRC receiver in asynchronous networks, a homogeneous network deployment is assumed, since the low power nodes in the heterogeneous network are synchronized with the macro eNodeBs, which is not the main focus of the paper. Furthermore, in the evaluation, the cell radius is set to be small to assess the urban area where higher performance is required compared to rural areas. In the paper, a multi-cell link simulation is conducted. The channel model is assumed to be a 6-ray typical urban (TU) channel model [12]. In the evaluation, the number of the transmitter and receiver antenna branches is assumed to be two and two, respectively. The transmitter and receiver spatial correlations are assumed to be 0.5. Four consecutive RBs are assigned to the UE. However, the covariance matrix estimation is limited within one RB since the UE is not always allocated to consecutive RBs. Therefore, the number of averaging samples, N_{sp}, equals 12 (this is the number of DM-RSs within 1 RB). A link-level simulation is performed between each UE and its serving cell as well as the neighboring cells. Regarding the CRS, we assume that the multicast/broadcast over single-frequency network (MBSFN) subframes [13] are configured, i.e., the CRS is transmitted only in the control region. In the evaluation, the two transmitter antenna branch codebooks defined in the LTE are used for precoding transmissions. Based on the CSI estimated using the CSI-RS, the UE selects the precoding weight matrix that maximizes the received signal-to-interference plus noise power ratio (SINR) from the codebook, and then the selected precoding weight matrix information at the UE is fed back to the serving cell without error. Note that the precoding weight matrix is randomly selected from the codebook for every subframe in the other interfering cells in the evaluation for simplicity. The channel estimation schemes for the CSI-RS and DM-RS are assumed to be the frequency-domain MMSE channel estimation [14] and the 2-dimensional MMSE channel estimation scheme [14], respectively. Note that a uniform delay power spectrum within the cyclic prefix length of 4.69 μsec and a uniform Doppler power spectrum with the maximum Doppler frequency of 5.55 Hz are assumed for the MMSE channel estimation filter. Hybrid auto repeat request (ARQ) using Chase combining is employed. In this paper, the asynchronous network is evaluated in addition to the synchronous network. When the cell(s) are asynchronous to the serving cell, the transmission timings of the asynchronous cell(s) are determined randomly at the fast Fourier transform (FFT) sample level. In order to evaluate the impact on asynchronous networks, the block error rare (BLER) performance for the IRC receiver is evaluated in two, three, and four-cell model environments where the average received signal-to-interference power ratio (SIR) is assumed to be a parameter. Here, the average received interference power is defined as the total interference power from interfering cells in this evaluation. Furthermore, in order to clarify the gain from the IRC receiver in the asynchronous networks, we evaluate the user throughput performance in a 57-cell model environment assuming a cellular environment in the LTE-Advanced downlink. The other link-level simulation conditions are given in Table I.

In the evaluation in the two, three, or four-cell model environments, we assume that the average received SIR equals 0 dB. The average received interference power from each interfering cell is assumed to be the same. The number of transmission streams is set to one for all cells.

In the evaluation in the 57-cell model environment, the cell layout is assumed to be a hexagonal grid, assuming 19 cell sites with 3 cells per site. The inter-site distance is assumed to be 500 m. We assumed 3 network models assuming the number of synchronous cells as the parameter, i.e., 3, 9, or 57 cells. Specifically, the cases for the number of synchronous cells of 3 and 9 are illustrated in Fig. 3. When the number of synchronous cells equals 3 or 9, we assume that the

TABLE I. LINK-LEVEL SIMULATION CONDITIONS

Carrier frequency / System bandwidth	2 GHz / 5 MHz
Maximum Doppler frequency	5.55 Hz
Number of transmitter antenna branches	2
Number of receiver antenna branches	2
Maximum number of transmission streams	2
Modulation and coding scheme	QPSK (R=1/3 – 5/6) 16QAM (R=1/2 – 5/6) 64QAM (R=3/5 – 4/5)
Number of allocated RBs	4 RBs (contiguous allocation)
Precoding / feedback granularity	4 RBs
Channel estimation for CSI-RS / DM-RS	Ideal or Freq. domain / 2D-MMSE channel estimation
HARQ (Round trip delay)	Chase combining (8 ms)

asynchronous networks where only the 3 cells within an eNodeB or the 9 cells within a cluster consisting of an eNodeB and 2 remote radio heads (RRHs) that are connected to the eNodeB by optical fiber are synchronized. On the other hand, when the number of synchronous cells equals 57, we assume a synchronous network among all cells. In the evaluation, one UE is selected randomly from the UEs that are uniformly distributed in the cell. Outer-loop link adaptation (OLLA) [15] is employed with the target BLER of 10%. In this paper, the UE throughput is obtained by averaging 400 subframes. The maximum number of streams is assumed to be 2 for all cells and the number of streams is determined adaptively every 400 subframes. The hard handover hysteresis is set to 3 dB in the evaluation. The other simulation conditions regarding the 57-cell model environment are given in Table II.

IV. PERFORMANCE EVALUATION

A. *Evaluation in Two, Three, and Four-Cell Model Environments*

The residual BLER performance is evaluated according to the number of interfering cells in the synchronous and asynchronous networks. Note that the residual BLER is defined as the value of the total error blocks after re-transmission divided by the total transmitted blocks. In this evaluation, the maximum number of re-transmissions is assumed to be one, the modulation and coding scheme is assumed to be QPSK with the coding rate of 1/2, and realistic channel estimations for the CSI-RS and DM-RS are assumed. Fig. 4 shows the residual BLER performance for each environment. For comparison, the simplified MMSE receiver is also evaluated.

We first compare the performance of a synchronous network. When the number of cells is two, i.e., only one interfering cell exists, the performance of the IRC receiver is improved compared to that of the simplified MMSE receiver, and an error floor is not observed. This is because one degree of freedom for the IRC receiver that has two receiver antenna branches is sufficient to suppress one interfering cell, i.e., one source of interference. In contrast, when the number of interfering cells is increased, the error floor is observed, and the error floor becomes higher. However, the performance improvement is still observed even when the number of interfering cells exceeds the degrees of freedom. This is because the IRC receiver tries to form the null beam toward the dominant interference at the time when generating the weight matrix, and to maximize the output SINR.

Next, we compare the performance of an asynchronous network. The results show that the performance of the IRC

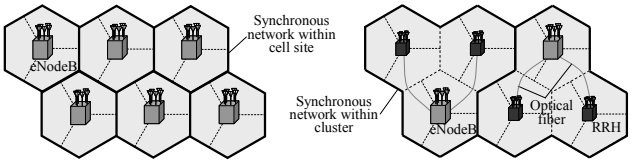

(a) Number of synchronous cells = 3 (b) Number of synchronous cells = 9

Figure 3. Asynchronous network model.

TABLE II. SIMULATION CONDITIONS FOR 57-CELL ENVIRONMENT

Inter-site distance	500 m
Distance dependent path loss	128.1 + 37.6log$_{10}$(r) dB (r in km)
Shadowing standard deviation	8 dB
Shadowing correlation	0.5 (Inter-site) / 1.0 (Intra-site)
Penetration loss	20 dB
Total transmission power	43 dBm
Transmitter antenna pattern (Antenna gain)	70-degree sectored beam (14 dBi) With tilt (θ_{etilt} = 15 degrees)
UE antenna gain / UE noise figure	0 dBi / 9 dB
Thermal noise density	-174 dBm /Hz
CSI-RS duty cycle configuration	10 ms interval
Hard handover hysteresis	3 dB

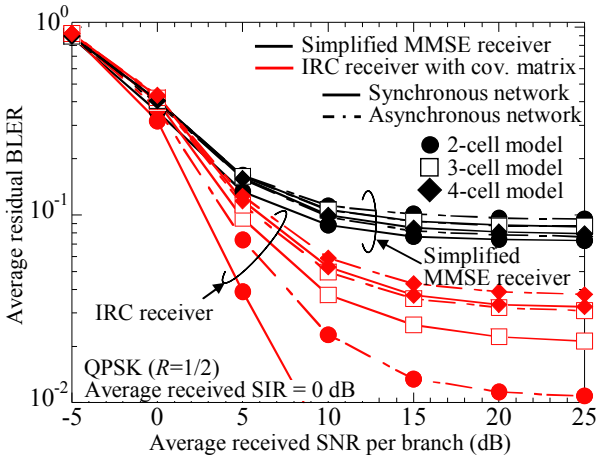

Figure 4. Residual BLER performance.

receiver is severely degraded in the high SNR region due to the asynchronous network even when the two-cell model environment is employed compared to that in the synchronous network. This is because the number of sources of interference is equivalently increased as discussed in Section II-C. However, in the three and four-cell model environments, the performance degradation between the synchronous and asynchronous networks becomes small. This is because the number of sources of interference which the IRC receiver tries to suppress far exceeds the degrees of freedom assuming two receiver antenna branches for both synchronous and asynchronous networks. However, even in the four-cell model environment, the gain from the IRC receiver is still observed for both networks.

Note that the performance for the simplified MMSE receiver is almost the same even if the number of interfering cells is increased. This is because the simplified MMSE receiver cannot suppress any sources of inter-cell interference.

Here, although the evaluation results are obtained by computer simulation in this section, the verification using the numerical analysis is shown in the appendix.

B. *Evaluation in 57-Cell Model Environment*

The performance is evaluated in the 57-cell model environment assuming a cellular environment. Before discussing the throughput performance, the interference profile is evaluated to understand the statistics of the interference. To this end, the dominant interferer proportion (DIP) [16] is used. After the location of the UE is randomly generated assuming a uniform distribution, the path loss including distance-dependent path loss and shadowing from 57 cells is calculated. The cell with the smallest path loss, i.e., highest received signal power is defined as the serving cell. Here, in order to include the handover hysteresis with 3 dB, when there are cells whose path loss is within 3 dB compared to that from the cell with the lowest path loss, the serving cell is randomly selected with the same probability from these cells. The 0-th cell (i = 0) is defined as the serving cell, and the i-th strongest cell except for the serving cell (i = 1, 2, …, N_{Cell}-1) is defined as an interfering cell. The i-th DIP, DIP_i, is defined as the average received power from the i-th interfering cell to the total interference plus noise power ratio, i.e., $DIP_i = \bar{P}_i \Big/ \left(\sum_{j=1}^{N_{\text{Cell}}-1} \bar{P}_j + \sigma^2\right)$. Here, $\bar{P}_i$ is the average received power from the i-th interfering cell. Furthermore, when the transmission timing of the i-th interfering cell is the same as that for the serving cell, the i-th DIP is regarded to be synchronized with the serving cell. In the evaluation, this process is repeated 30,000 times to obtained the cumulative distribution function (CDF). Figure 5 shows the CDF performance of the DIP for all the UEs. In this evaluation, the maximum number for i is set to 5 ($1 \le i \le 5$). The results show that the median DIP value (that is, the DIP value at the CDF of 50%) of the most dominant source of inter-cell interference is approximately -3 dB, which indicates that the most dominant source of inter-cell interference occupies approximately 50% of the total interference level. Furthermore, the median DIP value of the second dominant source of inter-cell interference is approximately -7 dB, which is only 4 dB lower than that of the most dominant source of inter-cell interference. Therefore, we can say that there are two dominant interfering cells. Note that for the IRC receiver that has two receiver antenna branches assumed in this paper, the sources of interference exceed the degrees of freedom at the receiver even when the number of streams at all the interfering cells is assumed to be one. In this case, clearly based on the performance results of the BLER evaluated in the previous section, the impact on the asynchronous network is small. Therefore, in the 57-cell model environment, we expect that this impact is also small. Regarding the i-th DIP, the probability that the i-th cell is synchronized with the serving cell is evaluated in asynchronous networks. Table III summarizes the results of the probability of synchronization with the serving cell for the dominant interfering cell in each DIP when the number of synchronous cells is 3 and 9. From these results, the probability that the two dominant interfering cells are synchronized with the serving cell is more than 50% even when the number of synchronous cells is assumed to be 3, i.e., the case where the number of synchronized cells is minimized is assumed. Therefore, we expect that the impact on the asynchronized cells is small

Finally, Table IV shows the cell-edge user throughput defined as the user throughput at the CDF of 5% and the average user throughput according to the number of synchronous cells. Note that the maximum number of re-transmissions is assumed to be three in this evaluation. From the results, the gain of the IRC receiver can be obtained even when the asynchronous network is assumed. Furthermore, from the viewpoint of the cell-edge user throughput, a gain exceeding 20% is achieved by the IRC receiver regardless of the number of synchronous cells. The reason why the throughput performance is not severely degraded especially at the cell edge in the asynchronous networks is that there are fewer degrees of freedom at the receiver than dominant sources of inter-cell interference in the 57-cell environment as described in the DIP performance evaluation. Under this condition, although the number of sources of interference is equivalently increased to generate the IRC receiver weight matrix in the asynchronous network, this impact does not severely affect the throughput performance.

Based on the above observations, the IRC receiver that has two receiver antenna branches can effectively suppress the inter-cell interference even when an asynchronous network is employed.

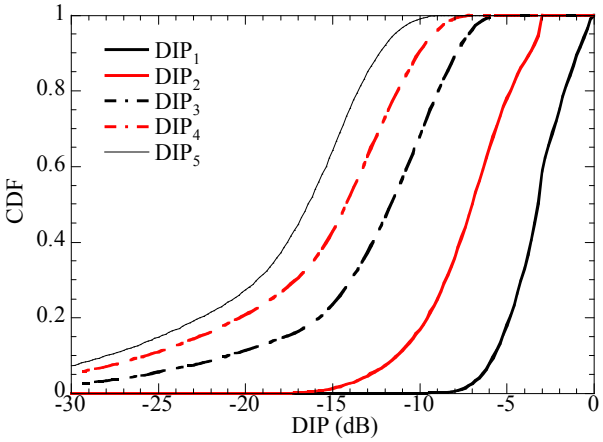

Figure 5. DIP performance.

TABLE III. PROBABILITY OF SYNCHRONIZATION WITH SERVING CELL FOR EACH DIP

Number of Synchronous Cells	DIP_1	DIP_2	DIP_3	DIP_4	DIP_5
3 cells	50.6%	57.1%	34.8%	22.9%	13.1%
9 cells	66.7%	71.1%	55.9%	47.5%	39.9%

TABLE IV. USER THROUGHPUT PERFORMANCE

		Number of Synchronous Cells		
		3 cells within cell site	*9 cells within cluster*	*57 cells (Sync. NW)*
Cell-edge user throughput	Simplified MMSE receiver (Mbps)	0.185	0.184	0.184
	IRC receiver (Mbps)	0.224 (+21.5%)	0.225 (+22.5%)	0.225 (+22.6%)
Average user throughput	Simplified MMSE receiver (Mbps)	1.119	1.119	1.124
	IRC receiver (Mbps)	1.192 (+6.6%)	1.194 (+6.6%)	1.201 (+6.8%)

(± *x*%): Relative gain compared to simplified MMSE receiver

V. CONCLUSION

In this paper, the performance of the IRC receiver in asynchronous networks was investigated using a multi-cell link simulation that could evaluate the actual estimation errors of the channel matrix and the covariance matrix. The simulation results showed that the impact on the asynchronous network

was large when the number of interfering cells was limited, i.e., the number of sources of interference did not exceed the degrees of freedom at the receiver. However, according to the increase in the number of interfering cells, the performance degradation due to the asynchronous network became small. Assuming the 57-cell model environment and a cellular environment in the LTE-Advanced downlink, the IRC receiver that has two receiver antenna branches could effectively suppress the inter-cell interference even when the asynchronous network was employed.

REFERENCES

[1] 3GPP, TS36.201 (V8.1.0), "LTE physical layer - general description," Nov. 2007.

[2] http://www.nttdocomo.com/pr/2010/001494.html

[3] 3GPP, TR36.913 (V8.0.0), "Requirements for further advancements for Evolved Universal Terrestrial Radio Access (E-UTRA) (LTE-Advanced)," June 2008.

[4] 3GPP, TR 36.814 (V1.0.0), "Further advancements for E-UTRA physical layer aspects," Jan. 2009.

[5] J. Winters, "Optimum combining in digital mobile radio with cochannel interference," *IEEE J. Sel. Areas Commun.*, vol. SAC-2, no. 4, pp. 528–539, July 1984.

[6] 3GPP, RP-111378, NTT DOCOMO, "Enhanced performance requirement for LTE UE," Sept. 2011.

[7] C.-H. Yu and O. Tirkkonen, "Characterization of SINR uncertainty due to spatial interference variation," in *Proc. SPAWC2010*, pp. 1-5, June 20-23, 2010.

[8] Y. Ohwatari, N. Miki, T. Asai, T. Abe, and H. Taoka, "Performance of advanced receiver employing interference rejection combining to suppress inter-cell interference in LTE-Advanced downlink," in *Proc. VTC2011-Fall*, Sept. 2011.

[9] L. Thiele, M. Schellmann, T. Wirth, and V. Jungnickel, "On the value of synchronous downlink MIMO-OFDMA systems with linear equalizers," in *Proc. IEEE ISWCS '08*, pp. 428-432, Oct. 21-24, 2008.

[10] 3GPP, R1-111562, Renesas Mobile Europe Ltd., "Interference aware receiver modeling at system level," May 2011.

[11] 3GPP, TR25.913 (V8.0.0), "Requirements for Evolved UTRA (E-UTRA) and Evolved UTRAN (E-UTRAN)," Jan. 2009.

[12] 3GPP, TS 45.005 (V5.4.0), "Radio transmission and reception," June 2002.

[13] 3GPP, TS36.211 (V10.2.0), "Physical channels and modulation," June 2011.

[14] P. Hoeher, S. Kaiser, and P. Robertson, "Two-dimensional pilot-symbol-aided channel estimation by Wiener filtering," in *Proc. ICASSP '97*, pp. 1845-1848, Apr. 1997.

[15] J. Lee, R. Arnott, K. Hamabe, and N. Takano, "Adaptive modulation switching level control in high speed downlink packet access transmission," in *Proc. 3G Mobile Communication Technologies 2002*, pp. 156-159, May 2002.

[16] 3GPP, TR25.963 (V10.0.0), "Feasibility study on interference cancellation for UTRA FDD User Equipment (UE)," April 2011.

APPENDIX

In order to verify the output SINR performance obtained by computer simulation, we also evaluate the performance obtained by numerical analysis. In [5], the CDF of the output SINR for the receiver employing optimum combining was derived analytically when assuming only one source of interference. Note that the receiver employing optimum combining is the same as the IRC receiver using the ideal channel and covariance matrices. When the uncorrelated receiver antenna branches and a flat fading channel model are assumed, the CDF of the output SINR is given by

$$P(\gamma) = \int_0^{\gamma/\Gamma_d} \frac{e^{-x} x^{N_{\mathrm{Rx}}-1}(1+N_{\mathrm{Rx}}\Gamma_1)}{(N_{\mathrm{Rx}}-2)!} \int_0^1 e^{-xN_{\mathrm{Rx}}\Gamma_1 t}(1-t)^{N_{\mathrm{Rx}}-2} dt dx , \qquad \text{(A1)}$$

where γ, Γ_d, and Γ_1 are the value of the output SINR, the average received SNR, and the average received interference–to-noise power ratio (INR), respectively. When assuming two or more sources of interference, Winters [5] claimed that it is extremely difficult to determine analytically the performance. Therefore, we only focus on a case with one source of interference in this appendix. Figure A1 shows the CDF of the output SINR obtained by (A1) assuming that Γ_d and Γ_1 equal 20 dB. Furthermore, the performance of the IRC receiver obtained by computer simulation is shown in this figure. Note that the simulation parameters basically follow those in Table I. However, to align the conditions of the derivation of (A1), the uncorrelated transmitter and receiver antenna branches and a flat fading channel model are assumed in the simulation. Additionally, the precoding weight matrix is assumed to be fixed in order to exclude the precoding gains for the performance. Regarding the models of the IRC receiver in the simulation, we evaluated the IRC receiver using a realistic channel and covariance matrix estimation (referred to as a realistic IRC receiver in this appendix) in addition to the ideal IRC receiver using the ideal channel and covariance matrices. For the realistic IRC receiver, we assume both synchronous and asynchronous networks and that the output SINR is defined as the averaged output SINR per RE on a logarithmic scale within 4 RBs, i.e., the allocated RBs for the UE. Furthermore, assuming an asynchronous network, the transmission timing of the OFDM symbols between the serving cell and the interfering cell is synchronized for simplicity although the delay times in the interfering cell are randomly set. Both the numerical analysis and simulation results of the ideal IRC receiver show that the performance levels are almost the same, and verify the output SINR performance obtained by computer simulation. From the viewpoint of the performance of the realistic IRC receiver, the performance for the synchronous network is slightly degraded compared to the ideal IRC receiver due to estimation errors. In contrast, it is shown that the performance for the asynchronous network is further degraded. The reason why this degradation occurs is mainly due to covariance matrix estimation errors caused by the asynchronous network as described in (7).

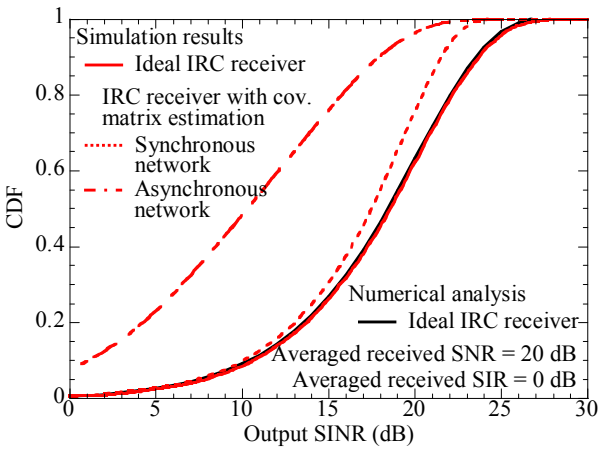

Figure A1. CDF of output SINR.